Clim. Past Discuss.,
https://doi.org/10.5194/cp-2019-146-AC2, 2020

Climate of the Past Discussions

Interactive comment on "Sequential changes in ocean circulation and biological export productivity during the last glacial cycle: a model-data study" *by* Cameron M. O'Neill et al.

Cameron M. O'Neill et al.

cameron.oneill@anu.edu.au

Received and published: 11 June 2020

CP reviewer comments #2 and author responses

AC: We thank the reviewer for their comments, suggestions and input into this manuscript. These comments make a substantial contribution to improving the quality of our work, particularly with reference to our treatment of the oceanic δ13C data. Please see below our responses to the individual comments.

We have made reference to changes to the manuscript, which are included as a supplement to the author comments, in track changes. Page and line references below

refer to locations in the revised document with track changes.

RC 1. The authors base their paper on a recently published carbon cycle box model (O'Neill et al. 2019). They provide a brief description of the model but I found that this manuscript would benefit better description of some of the key parameters that are quite important to this paper, such as the controls on Z (biological productivity). It was very unclear to me on first reading how values of Z were ascertained.

AC: To address this comment we have added the following text to (P3, L30). In addition to the biological productivity, it includes a bit more detail on some other processes, stemming from the other reviewer comments:

"We used the SCP-M carbon cycle box model in our model-data experiment (O'Neill et al., 2019). In summary, SCP-M contains simple parameterisations of the major fluxes in the Earth's surface carbon cycle (Fig. 1). SCP-M incorporates the ocean, atmosphere, terrestrial biosphere and marine/continental sediment carbon reservoirs, weathering and river fluxes, and a number of variables including atmospheric CO2, DIC, phosphorus, alkalinity, carbon isotopes (13C and 14C) and the carbonate ion.

SCP-M calculates ocean pCO2 using the equations of Follows et al. (2006), and applies the first and second "dissociation constants" of carbonic acid estimated by Lueker et al. (2000), to calculate HCO $-$ and CO2$-$3 concentrations, respectively, in units of μmol kg$-$1, in each ocean box. The model employs partial differential equations for determining the concentration of elements in each box, with each box represented as a row and column in a matrix. In this paper, we extend SCP-M by incorporating a separate basin for the combined Pacific and Indian Oceans (Fig. 1), following the conceptual model of Talley (2013), to incorporate modelling and proxy data for those regions of the ocean. This version of SCP-M consists of 12 ocean boxes plus the atmosphere and terrestrial biosphere. SCP-M splits out depth regions of the ocean between surface boxes (100-250m average depth), intermediate (1,000m average depth), deep (2,500m average depth) and abyssal depth boxes (3,700 (Atlantic) - 4,000m (Pacific-

Indian) average depth). The Southern Ocean is split into two boxes, including a polar box which covers latitude range 60-80 degrees South (box 12 in Fig. 1) and sub polar boxes in the Atlantic (box 7) and Pacific-Indian (box 12) basins, which cover latitude range 40-60 degrees South. See O'Neill et al. (2019) for a discussion of the choice of box depth and latitude dimensions.

The major ocean carbon flux parameters of interest in this model-data study, are global ocean circulation (GOC), $\Psi 1$, Atlantic meridional overturning circulation (AMOC), $\Psi 2$, and ocean biological export productivity, Z. The ocean circulation parameters $\Psi 1$ and $\Psi 2$ are simply prescribed in units of Sverdrups (Sv, 106 m3 $s-1$). Ocean biological export productivity Z is calculated using the method of Martin et al. (1987). The biological productivity flux, at 100m depth, is attenuated with depth for each box according to the decay rule of Martin et al. (1987). Each sub surface box receives a biological flux of an element at its ceiling depth, and loses a flux at its floor depth (lost to the boxes below it). The difference is the amount of element that is remineralised into each box. The input parameter is the value of export production at 100m depth, in units of mol C $m-2$ $yr-1$ as per Martin et al. (1987). Equation (1) shows the general form of the Martin et al. (1987) equation:

F=F100(d/100)b (1)

Where F is a flux of carbon in mol C $m-2$ $yr-1$, F100 is an estimate of carbon flux at 100m depth, d is depth in metres and 20 b is a depth scalar. In SCP-M, the Z parameter implements the Martin et al. (1987) equation. Z is an estimate of biological productivity at 100m depth (in mol C $m-2$ $yr-1$), and coupled with the Martin et al. (1987) depth scalar, controls the amount of organic carbon that sinks from each model surface box to the boxes below. Each subsurface ocean box receives a flux of carbon from the box above it, at its ceiling depth (also the floor of the overlying box), and loses carbon as a function of the depth of the bottom of the box. Remineralisation in each box is accounted for as the difference between the influx and out-flux of organic carbon.âĂĺ The terrestrial biosphere is represented in SCP-M as a stock of carbon (a box) that

fluxes with the atmosphere, governed by parameters for net primary productivity (NPP) and respiration. In SCP-M, NPP is calculated as a function of carbon fertilisation, 25 which increases NPP as atmospheric CO2 rises via a simple logarithmic relationship, using the model of Harman et al. (2011). This is a simplified approach, which omits the contribution of temperature and precipitation on NPP. Other, more complex models of the carbon cycle applied to glacial-interglacial cycles have a more detailed treatment of the terrestrial biosphere, including climate dependencies (e.g. Brovkin et al., 2002; Menviel et al., 2012). A number of studies emphasise the role of atmospheric CO2 as the driver of terrestrial biosphere NPP on glacial-interglacial cycles (Kaplan et al., 2002; Otto et al., 2002; 30 Joos et al., 2004; Hoogakker et al., 2016), although other studies cast doubt on the relative importance of atmospheric CO2 versus temperature and precipitation (Francois et al., 1999; van der Sleen, 2015).âĂĺ

The isotopic fractionation behaviour of the terrestrial biosphere may also vary on glacial-interglacial timeframes. This has been studied for the LGM, Holocene and the present day (e.g. Collatz et al., 1998; Francois et al., 1999; Kaplan et al., 2002; Kohler and Fischer, 2004; Joos et al., 2004; Kohn, 2016). The variation in isotopic fractionation within the terrestrial biosphere reflects changes in the relative proportions of plants with the C3 and C4 photosynthetic pathways, but also strong variations within the same photosynthetic pathways themselves (Francois et al., 1999; Kohn, 2010; Schubert and Jahren, 2012; Kohn, 2016). The drivers for these changes include relative sea level and exposed land surface area (Francois et al., 1999), global tree-line extent (Kohler and Fischer, 2004), atmospheric temperature and CO2 (Collatz et al., 1998; Francois et al., 1999; Kohler and Fischer, 2004; Kohn, 2010; Schubert and Jahren, 2012), global and localised precipitation and humidity (Huang et al., 2001; Kohn, 2010; Schubert and Jahren, 2012; Kohn, 2016), and also changes in the intercellular CO2 pressure in the leaves of C3 plants (Francois et al., 1999). Estimated changes in average terrestrial biosphere δ13C signature between the LGM and the Holocene fall in the range -0.3-1.8‰ (less negative δ13C signature in the LGM), with further changes estimated from the onset of the Holocene to the pre-industrial, and even greater changes to the present

day (due to rising atmospheric CO2). This feature has been covered in detail within studies that focussed on the terrestrial biosphere between the LGM and Holocene, but less so in modelling and model-data studies of the last glacial-interglacial cycle. Menviel et al. (2016) provided a sensitivity of -0.7+0.5‰ around an average LGM terrestrial biosphere value δ13C of -23.3‰ based on previous modelling of the LGM-Holocene timeframe by Joos et al. (2004). Another modelling study (Menviel and Joos, 2012), assessed the variation in LGM-Holocene δ13C of the terrestrial biosphere to be a minor factor and it was omitted. Kohler and Fischer (2004) assessed the changing δ13C signature of plants between the LGM and Holocene to be a minor factor in setting δ13C of marine DIC, compared to changes in the absolute size of the terrestrial biosphere across this period. Given the uncertainty and ranges of starting estimates of terrestrial biosphere δ13C, the uncertain LGM-Holocene changes, the large number of potential drivers, and the further uncertainty in extrapolating the posited LGM-Holocene changes back for the preceding 100 kyr, and the modest changes relative to the average δ13C signature (and the very large range in, for example, present day estimates of C3 plant δ13C (Kohn, 2010, 2016), we omit this feature with the caveat that there is added uncertainty in our terrestrial biosphere results with respect of the δ13C signature applied. We apply an average δ13C signature of -23‰ similar to values assumed by Menviel et al. (2016) and Jeltsch-Thommes et al. (2019) (23.3‰ -24‰ respectively), but more negative than assumed in Brovkin et al. (2002), Kohler and Fischer (2004) and Joos et al. (2004) (-16-(-17)‰. Our aim is not to contribute new findings of the terrestrial biosphere, but to ensure that the simple representation of the terrestrial biosphere in SCP-M provides the appropriate feedbacks to our (exhaustive) glacial-interglacial cycle model-data optimisation experiments, that are in line with published estimates. Air-sea gas exchange is based on the relative pCO2 in the surface ocean boxes and the atmosphere, and a parameter that 30 sets its rate in m day$-$1, P (Fig. 1).

pCO2 is calculated using the method of Follows et al. (2006). SCP-M represents ocean carbonate chemistry with a parameterisation of shallow water carbonate production, linked to the Z parameter by an assumption for the relative proportion of car-

bonate vs organic matter, known as "the rain ratio" (e.g. Archer and Maier-Reimer, 1994; Ridgwell, 2003). Carbonate dissolution is calculated based on the ocean box or marine surface sediment calcium carbonate concentration versus a depth-dependant saturation concentration (Morse and Berner, 1972; Millero, 1983). Most other carbon 35 cycle processes are parameterised simply, such as volcanic emissions, continental weathering, anthropogenic emissions and cosmic 14C fluxes. The isotopes of carbon are calculated applying various fractionation factors associated with the biological, physical and chemical fluxes of carbon (O'Neill et al., 2019).

We have added a simple representation of shallow water carbonate fluxes of carbon and alkalinity in SCP-M's low latitude surface boxes, to cater for this feature in theories for glacial cycle CO2 (e.g. Berger, 1982; Opdyke and Walker, 1992; Ridgwell et al., 2003; Vecsei and Berger, 2004; Menviel and Joos, 2012), using:

dCi /dt reef = Creef /Vi (2) âĂĺ

Where Creef is the prescribed flux of carbon out of/into the low latitude surface ocean boxes during net reef accumula- tion/dissolution, in mol C yr$-$1, and Vi is the volume of the low latitude surface box i. The alkalinity flux associated with reef production/dissolution is simply Eq. 2 multiplied by two (e.g. Sarmiento and Gruber, 2006).

The major fluxes of carbon are parameterised simply in SCP-M to allow them to be solved by model-data optimisation with respect of atmospheric and ocean proxy data. In this study, the values for GOC, AMOC and biological export productivity at 100m depth, are outputs of the model-data experiments, as they are deduced from a data optimisation routine. Their input values for the experiments are ranges, as described in 2.2.1. SCP-M's fast run time and flexibility renders it useful for long term paleoreconstructions involving large numbers of quantitative experiments and data integration (O'Neill et al., 2019). SCP-M is a simple box model, which incorporates large regions of the ocean as averaged boxes and parameterised fluxes. It is an appropriate tool for this study, in which we evaluate many tens of thousands of simulations to

explore possible parameter combinations, in conjunction with proxy data. The model used for this paper is located at https://doi.org/10.5281/zenodo.3559339.âĂĺ

RC: Figure 1 – this graphic, while nice and colourful, is challenging for reading the actual numbers and symbols (especially the white ones which do not show up at all on my colour print). Readability is more important than colour! I suggest making box numbers, symbols all BLACK using larger fonts so that they are readable.

AC: Thanks. To address this comment, for Figure 1 we have upgraded the box number font size, in bold and black, and we increased font sizes for text elsewhere in the diagram. We would like to retain the colour coding of parameter symbols with their associated flux arrows. To address the RC, we have expanded the font size of these to help with readability (please see attached revised manuscript at Figure 1).

RC: Pg 5 lines 15-17. This sentence seems out of place: "Therefore, our modelling excludes the last glacial termination (âĹij11-18 ka)." Should it occur before the previous sentence?

AC: Thanks, we have relocated the misplaced sentence (P8, L14).

RC: Section 2.2.1 Model forcings: Although the authors ultimately conclude that sea ice cover – as a barrier mechanism constraining air-sea CO2 exchange – is not that important, the authors should emphasize limitations of their use of the ice core sea ice proxy. First, this proxy is non-linear, so their simulations probably over estimate early (MIS5d) sea ice cover and underestimate later (MIS4-2) sea ice cover. This point is made very clearly by Wolff et al. 2010 (and supports) the authors' assertion that the barrier effect of sea ice early in the glaciation is probably small.

Text added in the methodology section (P8, L28).

"Our treatment of sea-ice cover is simply as a regulator of air-sea gas exchange in the polar ocean surface boxes. This treatment misses important linkages that likely exist between sea-ice cover and Southern Ocean upwelling, wind-sea surface interactions,

NADW formation, deep ocean stratification, nutrient distributions and biological productivity (Morrison and Hogg, 2013; Ferrari et al., 2014; Jansen, 2017; Kohfeld and Chase, 2017; Marzocchi and Jansen, 2017). Furthermore, our linear application of the sea-ice proxy data of Wolff et al. (2010) to our air-sea gas exchange parameter may serve to overestimate its effect on the model results early in the glacial period (MIS 5d), and underestimate it during MIS 2-4 (Wolff et al., 2010)."

RC: Furthermore, it is worth pointing out somewhere in the discussion that this modelling exercise only examines the potential role of sea ice as a barrier to CO2 exchange, and not its synergistic (and likely more important) roles in influencing nutrient distributions, marine productivity, and a trigger for deep ocean circulation changes. The authors state this somewhat in their "Advantages and limitations" section, but I think that this point could be made more explicitly.

AC: To address this comment, we have added the following (P27, L23):

"This finding may reflect our approach to treat polar sea-ice cover simply as a regulator of the rate of air-sea gas exchange in the polar oceans. This approach may neglect other effects of sea-ice cover including as a trigger for changes in Southern Ocean upwelling, NADW formation rates, deep ocean stratification, nutrient distributions and biological productivity (Morrison et al, 2011; Brovkin et al, 2012; Ferrari et al, 2014; Kohfeld and Chase, 2017; Jansen, 2017; Marzocchi and Jansen, 2017). For example, Brovkin et al (2012) found that in the CLIMBER-2 model, atmospheric CO2 was more sensitive to sea ice cover when it was linked to weakened vertical diffusivity in the Southern Ocean of tracers such as DIC, thereby reducing outgassing of CO2."

RC: Another larger issue that the sea ice proxy highlights is the spatial heterogeneity of the Southern Ocean and how the model results are linked with reality: the sea ice proxy likely represents changes very close to the continent and early glacial changes in sea ice are not well reproduced in the few long sea ice records that are found near the APF. This not only suggests that a barrier effect of sea ice would be limited to only part

of the Southern Ocean, it points to larger issues with treating the Southern Ocean as one box, with an unclear delineation of how much of the S. Oc. this box is presumed to cover. If the box is supposed to ONLY cover those areas close to the continent where AABW and Circumpolar Deepwater processes that influence GOC are most important, then the authors' main conclusion of increases in S. Oc. export production aren't well supported by paleoceanographic data which show reductions in export South of the APF for the majority of the glacial cycle between MIS5d and MIS2. Some discussion of what the Southern Ocean box actually represents - and this potential disconnect with paleoceanographic data - is warranted.

AC: SCP-M has two Southern Ocean boxes in each basin: a polar and sub polar Southern Ocean box. These are: polar Southern Ocean box for both basins (box 12 in Figure 1) which covers 60-80 deg S, sub polar Atlantic box (box 7 in Figure 1, 40-60 deg S) and sub polar Pacific-Indian box (box 11, 40-60 deg S). The sea ice forcing/air-sea gas exchange is undertaken for the polar Southern Ocean box. The biological export productivity experiment is undertaken for the sub polar Southern Ocean boxes in each basin, as per the regions highlighted for increased glacial period biological activity by Martinez-Garcia (2014) and Lambert et al (2015), Shoenfelt et al (2018). Put another way, our Southern Ocean biological flux experiments are not concerned with the APF, but with the open Southern Ocean box.

We have added the following text in the model description in Section 2.1 (P5, L6):

"The Southern Ocean is split into two boxes, including a polar box which covers latitude range 60-80 degrees South (box 12 in Fig. 1) and sub polar boxes in the Atlantic (box 7) and Pacific-Indian (box 12) basins, which cover latitude range 40-60 degrees South. See O'Neill et al (2019) for a discussion of the choice of box depth and latitude dimensions."

We have also added the following text in the first paragraph of Section 2.2.1 Model parameters and forcing (P8, L26):

"Note the polar Southern Ocean box which is forced with reduced air-sea exchange, is separate from the sub polar Southern Box in which the biological export productivity parameter is varied in the model-data experiment."

RC: Throughout the paper the authors refer to "abyssal" and "deep" water masses for all basins, but I was never able to find the depth cut-offs that were used to distinguish these depths in the different basins. Please put them in the figure captions and text (not just supplemental information, if it is there.)

AC: We have added the following text in the model description in Section 2.1 (P5, L4):

"SCP-M splits out depth regions of the ocean between surface boxes (100-250m average depth), intermediate (1,000m average depth), deep (2,500m average depth) and abyssal depth boxes (3,700-4,000m average depth). The Southern Ocean is split into two boxes, including a polar box which covers latitude range 60-80 degrees South (box 12 in Fig. 1) and sub polar boxes in the Atlantic (box 7) and Pacific-Indian (box 12) basins, which cover latitude range 40-60 degrees South. See O'Neill et al (2019) for a discussion of the choice of box depth and latitude dimensions."

We have also added depth references to the Caption on Figure 1, Figures 5-7, Figures 9-11

RC: The authors discuss briefly that previous studies have only used the C. wuellerstorfi data to reconstruct deep ocean δ13C (Peterson et al. study; Kohfeld and Chase study). Which data did these authors select from Oliver et al. (2010)? They mention only using "deep" and "abyssal" sites (again, depths undefined) on page 11, but they do not indicate whether they have filtered the data to only include C. wuellerstorfi (or even Cibicidoides spp), which they SHOULD be doing if they haven't. Otherwise, the changes in δ13C described on page 12 are invalid as descriptions of deep ocean circulation changes in δ13C.

AC: The work of Oliver et al (2010) was to aggregate ocean δ13C data, estimate and

correct for species-related problems or errors, and thereby provide a dataset to be used for assessing ocean circulation changes. The Oliver et al (2010) dataset is split into Planktonic and Benthic species data. We had used the benthic datasets. We had given Oliver et al (2010) the benefit of the doubt, in our first manuscript, as they had gone to substantial effort to produce a δ13C dataset for paleooceanographic purposes.

However, on the suggestion of the reviewer, we have revisited the data and filtered the Cibicides species for the δ13C dataset, which also includes Cibicides data contributed by Govin et al (2009) and Piotrowski et al (2009).

We have re-constructed our ocean δ13C database using only the Cibicides species δ13C data, re-calibrated the model for a new set of (penultimate) interglacial starting data, and re-run all of our model-data experiments. The revised manuscript (attached) incorporates these changes in the text, charts and tables.

The data section is updated as follows (P13, L4):

"Oliver et al. (2010) compiled a global dataset of 240 cores of marine δ13C data encompassing benthic and planktonic species over the last âĹij150 kyrs. Oliver et al. (2010) observed considerable uncertainties associated with the broad range of species included, particularly for the planktonic foraminifera. By comparison, Peterson et al. (2014) aggregated marine δ13C for the LGM and late Holocene periods, as time period averages, exclusively sampling benthic C. wuellerstorfi data, which is a more reliable indicator of marine δ13C (Oliver et al., 2010; Peterson et al., 2014). To narrow the range of uncertainty, we constrain our use of marine δ13C data to the deep and abyssal benthic Cibicides species foraminifera samples in the Oliver et al. (2010) dataset, supplemented with Cibicides species δ13C proxy data from Govin et al. (2009) and Piotrowski et al. (2009) (Table 2). Figure 3 shows the δ13C data locations from Oliver et al. (2010), which are concentrated in the Atlantic Ocean. We mapped and averaged the carbon isotope data into SCP-M's boxes on depth and latitude coordinates (Fig. 1), and averaged for each MIS time slice."

RC: On Page 12, the authors qualitatively describe the differences between "deep" and "abyssal" changes in δ13C. Why leave this discussion qualitative, when the data are available and quantification would be hugely useful. These data in the Pacific that are described are the data that pin the authors' entire argument surrounding early changes in GOC. I think that this warrants a bit more quantification of these data (once species other than Cibicidoides are filtered out of the dataset). I would be interested to know if the differences between deep and abyssal δ13C in the Indo-pacific are statistically significant, and I think plots of the probability distribution functions of these data would be very useful.

AC: Thanks. Following from this comment we've investigated a number of ways to analyse the data. We have focussed on the δ13C data (Cibicides, as above) only, for this analysis, as there is continuous coverage for deep and abyssal boxes for the Atlantic and Pacific-Indian oceans across all of the MIS stages we are interested in.

We applied some tests for statistical significance of the various boxes throughout the MIS stages. We used a Welch's paired unequal variance t-test for statistically different mean δ13C between deep and abyssal boxes, and also for differences in the offsets in mean δ13C between deep and abyssal boxes, between MIS stages. We have added this to the supplementary information file and referenced its location from the main document (P17 L13).

As per the reviewer comment, we first plot the distribution of mean δ13C values for each of the deep and abyssal boxes across the MIS stages.

Figure 1: Distribution histograms of δ13C data for the Pacific-Indian (left column) and Atlantic Ocean (right column) deep (100/1,000-2,500m) and abyssal (>2,500m) boxes. Plots also show the mean δ13C for each box (vertical dashed lines), and the calculated offset between the deep and abyssal mean δ13C values (CP_RC2_Fig1.png). (see below for Figure 1)

We applied a Welch's paired t-test to test for statistical independence of the means of

δ13C in the deep and abyssal ocean boxes for Atlantic and Pacific-Indian, within each MIS. This returns p-values very close to zero for every box pair and every MIS. A p-value <0.05 means that we reject the null hypothesis that the abyssal and deep ocean boxes are statistically the same. That is, our deep and abyssal boxes in the model are statistically independent of each other, in terms of mean δ13C. This simply confirms that our abyssal and deep ocean boxes are not the same in terms of mean δ13C in each MIS.

Table 1: Tests for statistical independence of the mean δ13C between deep and abyssal boxes (CP_RC2_Tab1.png). (see below for Table 1)

Given we discuss in the manuscript (qualitatively) the changes in the offset between deep and abyssal ocean δ13C through the MIS, we can test to see if the changes in deep-abyssal offset from the penultimate interglacial (MIS 5e) to the glacial periods are statistically significant. The chart below shows the deep-abyssal offsets in δ13C for the Pacific-Indian and Atlantic Ocean boxes through each MIS of the last glacial-interglacial cycle. We show the absolute deep-abyssal δ13C offsets for Pacific-Indian and Atlantic Ocean boxes, for each MIS (columns). We also show the deep-abyssal δ13C offsets relative to the penultimate interglacial in MIS 5e (lines).

The Pacific-Indian δ13C offset shows a widening in MIS 5d, relative to MIS 5e, which is maintained until MIS 5a, and then begins a slow decline. The offset declines to a similar value to MIS 5e, by MIS 1 (the Holocene). The Atlantic deep-abyssal δ13C offset does not increase meaningfully until MIS 4, and then peaks at MIS 2 (the LGM), before contracting at MIS 1 to a value almost the same as MIS 5e.

Figure 2: Offsets between mean deep and abyssal box δ13C for each MIS in the last glacial-interglacial cycle for the Pacific-Indian (blue columns) and Atlantic Ocean (grey columns). Changes in the offsets from the penultimate interglacial (MIS 5e) are shown by the blue (Pacific-Indian) and grey (Atlantic) lines (CP_RC2_Fig2.png).(see below for Figure 2)

We further undertook Welch's paired T-tests for the independence of deep-abyssal offsets in mean δ13C with respect of the penultimate interglacial period (MIS 5e), for the periods MIS 1-5e. The null hypothesis is that the deep-abyssal offset in mean δ13C in each MIS is not statistically independent of MIS 5e (i.e. statistically the same and not supportive of a change in deep-abyssal δ13C distribution that may be delivered by a changed ocean process). p-values>0.05 lead to the null hypothesis being accepted, whereas p-values <0.05 lead to the null hypothesis being rejected and confirm statistical independence of the deep-abyssal offsets relative to MIS 5e (perhaps supportive of a changed ocean distributive process in the glacial period). Deep-abyssal offsets for the Pacific-Indian during MIS 2-MIS5d are statistically independent of MIS 5e, supportive of a changed oceanic distribution of δ13C throughout the glacial period. The MIS 1 Pacific-Indian deep-abyssal δ13C offset is not statistically independent of MIS 5e, indicating a similar deep-abyssal δ13C distribution between the last and penultimate interglacial periods. For the Atlantic Ocean, deep-abyssal mean δ13C offsets are not statistically independent with respect to MIS 5e (p-value >0.05, accept null hypothesis), until the period MIS 2-4. Atlantic deep-abyssal mean δ13C offset in MIS 1 is not statistically different from MIS 5e.

Table 2: Statistical tests for significance of difference in deep-abyssal δ13C offsets versus penultimate interglacial (MIS 5e). 'Accept'/red is to accept the null hypothesis - no statistically significant difference, 'Reject'/green is to reject the null hypothesis – statistically significant difference with respect of MIS 5e (CP_RC2_Tab2.png). (see below for Table 2)

The statistical analysis above is helpful and provides support for our model-data experiment results – that GOC slowed in MIS 5d and AMOC slowed in MIS 4. However, we do want to make the point that our model-data results don't hang on one particular data point to deliver these findings, in any MIS. They are constrained and optimised with many observations. The model-data results in the first instance are telling us that, the many observational forcings we have imposed in each MIS (SST, salinity, sea-ice

cover proxy, coral reef carbonates) are not enough to deliver the change in atmospheric CO2, atmospheric and ocean δ13C, D14C and CO23 proxy data. Changes from within the set of ocean circulation, mixing and/or biology parameters are needed. Note the result for GOC that is hinted at by the δ13C data, that we model in our experiments, is sustained throughout the last glacial cycle, not just at MIS 5d.

The main point of our work, and what has taken substantial effort, is to undertake an exhaustive model-data optimisation using a carbon cycle box model and multiple atmospheric and ocean proxy data. The model-data results don't just rely on one data point, the results need to be the best fit for all the data used, in each MIS. This is where this model-data experiment differentiates itself from many others.

We have included the distribution plot and T-test table above, in the manuscript's Supporting Information. We make reference to this material in the manuscript when discussing the data charts in the "Data Analysis" section. This chart/table provide supplemental support to the model-data analysis, the latter being the focus of our manuscript. We feel that the manuscript is becoming very voluminous and we also think that this analysis would require its own section in the manuscript (However, it is presented in this response to the discussion (preserved online) and in the SI).

RC: Some type of quantification would also be very useful for the authors' description of the "transient drop in abyssal Atlantic ocean CO3= at MIS5b" on page 14. I was not convinced that this transient drop exists from the figure presented.

AC: Yes, the axes on these charts are a little difficult to decipher small changes in the data. We wish to show the range of shallow-deep CO23 data (not just deep-abyssal), as the pattern is quite interesting at the LGM-Holocene. Our suggestion is to add the changes in units for the pattern that we wish to describe (P17, L35):

"There is a modest drop in abyssal Atlantic Ocean CO2-3 at MIS 5b (-13 μmol kg$-$1 relative to MIS 5c), which coincides with a minor drop in abyssal Atlantic Ocean δ13C (-0.19‰ and atmospheric CO2 (-14 ppm), suggesting a possible common link." RC:

Please note on the bottom of page 13 and top of page 14 that the authors mean to refer to Figure 7 (not 6) to describe carbonate ion concentration data.

AC: Thank you, we have corrected these references in the manuscript.

RC: Last sentence before Results section: Please cite the figures you are using to make these observations about changes in δ13C and DD14C

AC: We have added the figure references

RC: Similar quantification would be useful in the comparison between the carbonate ion concentration model output and data in Figure 9 and in the discussion on page 16-17.

AC: Figure references for Figure 9 added to the text here

âĂČ References

Govin, A., Michel, E., Labeyrie, L., Waelbroeck, C., Dewilde, F., and Jansen, E.: Evidence for northward expansion of Antarctic Bottom Water mass in the Southern Ocean during the last glacial inception, Paleoceanography, 24, doi:10.1029/2008PA001 603, 2009.

Lambert, F., Tagliabue, A., Shaffer, G., Lamy, F., Winckler, G., Farias, L., Gallardo, L., and Pol-Holz, D.: Dust fluxes and iron fertilization in Holocene and Last Glacial Maximum climates, Geophysical Research Letters, 42, 6014–6023, 2015.

Martinez-Garcia, A., Sigman, D., H.Ren, Anderson, R., Straub, M., Hodell, D., Jaccard, S., Eglinton, T., and Haug, G.: Iron Fertilization of the Subantarctic Ocean During the Last Ice Age, Science, 343, 1347–1350, 2014.

Oliver, K., Hoogakker, B., Crowhurst, S., Henderson, G., Rickaby, R., Edwards, N., and Elderfield, H.: A synthesis of marine sediment core d13C data over the last 150 000 years, Climate of the Past, 6, 645–673, 2010.

Piotrowski, A., Banakar, V., Scrivner, A., Elderfield, H., Galy, A., and Dennis, A.: Indian Ocean circulation and productivity during the last glacial cycle, Earth and Planetary Science Letters, 285, 179–189, 2009.

Shoenfelt, E.M., Winckler, G., Lamy, F., Anderson, R.F., and Bostick, B.C. Highly bioavailable dust-borne iron delivered to the Southern Ocean during glacial periods. PNAS 115 (44) 11180-11185, 2018. https://doi.org/10.1073/pnas.1809755115.

Please also note the supplement to this comment:
https://www.clim-past-discuss.net/cp-2019-146/cp-2019-146-AC2-supplement.pdf

Interactive comment on Clim. Past Discuss., https://doi.org/10.5194/cp-2019-146, 2019.

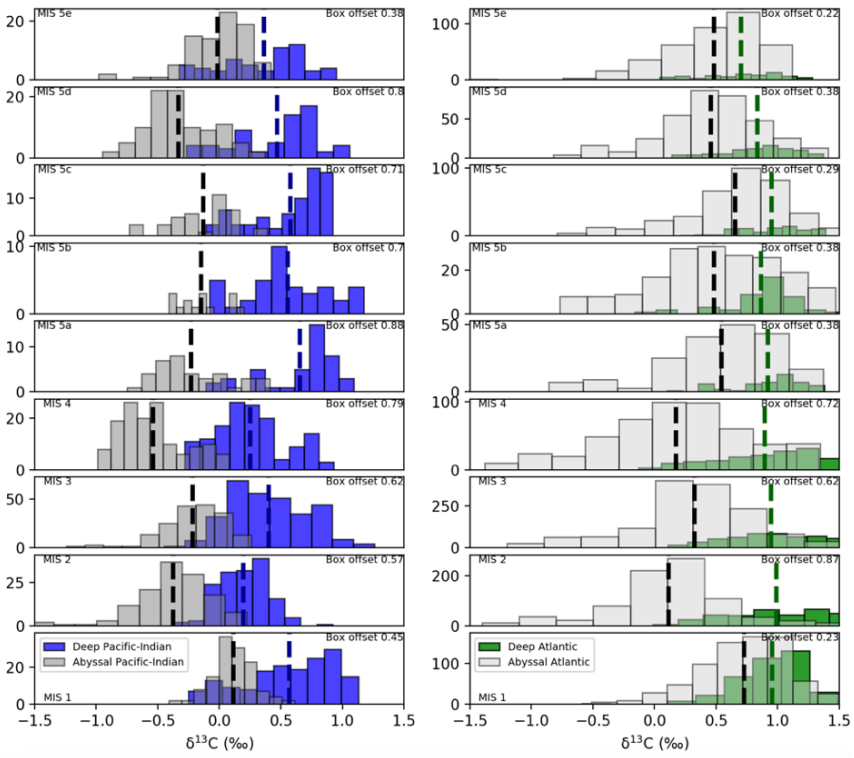

Fig. 1. Figure 1: Distribution histograms of δ13C data for the Pacific-Indian (left column) and Atlantic Ocean (right column) deep (100/1,000-2,500m) and abyssal (>2,500m) boxes. Plots also show the mean δ13C

MIS	Abyssal-deep Pacific-Indian		Abyssal-deep Atlantic	
	t-statistic	p-value	t-statistic	p-value
MIS5e	-7.0	0	5.1	0
MIS5d	16.1	0	9.8	0
MIS5c	13.0	0	7.8	0
MIS5b	9.5	0	6.3	0
MIS5a	13.2	0	6.9	0
MIS4	24.0	0	17.6	0
MIS3	23.3	0	21.6	0
MIS2	18.8	0	31.6	0
MIS1	14.2	0	11.9	0

Fig. 2. Table 1: Tests for statistical independence of the mean δ13C between deep and abyssal boxes (CP_RC2_Tab1.png)

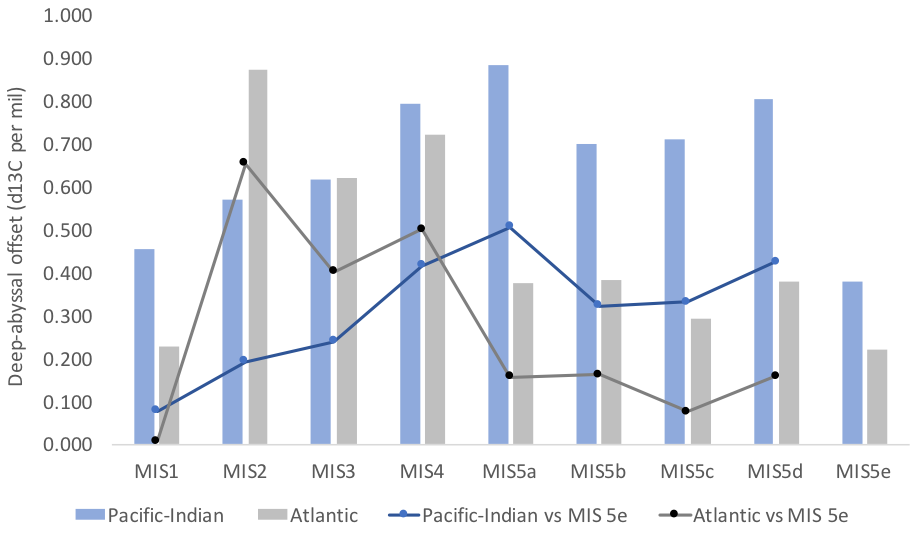

Fig. 3. Figure 2: Offsets between mean deep and abyssal box δ13C for each MIS in the last glacial-interglacial cycle for the Pacific-Indian (blue columns) and Atlantic Ocean (grey columns). Changes in the off

	Pacific-Indian (vs MIS 5e)			Atlantic (vs MIS 5e)		
MIS	t-statistic	p-value	Accept/ reject null	t-statistic	p-value	Accept/ reject null
MIS 5e	0.0	0.500	Accept	0.0	0.500	Accept
MIS5d	3.8	0.000	Reject	1.4	0.079	Accept
MIS5c	3.0	0.002	Reject	0.7	0.253	Accept
MIS5b	2.9	0.002	Reject	1.5	0.074	Accept
MIS5a	4.5	0.000	Reject	1.4	0.082	Accept
MIS4	3.7	0.000	Reject	4.5	0.000	Reject
MIS3	2.1	0.017	Reject	3.6	0.000	Reject
MIS2	1.7	0.044	Reject	5.9	0.000	Reject
MIS1	0.7	0.246	Accept	0.1	0.478	Accept

Fig. 4. Table 2: Statistical tests for significance of difference in deep-abyssal δ13C offsets versus penultimate interglacial (MIS 5e). 'Accept'/red is to accept the null hypothesis - no statistically signif